Development of Catalytic Alkylation and Fluoroalkylation Methods

Final Report

- **Grant Number**: DE-FG02-07ER15885
- **Previous Project Title**: Mild Catalytic Methods for Alkyl-Alkyl Bond Formation
- **Applicant/Institution**: David A. Vicic, Department of Chemistry, University of Hawaii, 2545 McCarthy Mall, Honolulu, HI 96822 Ph: (808) 956-2705. E-mail: vicic@hawaii.edu
- **Project performance site**: University of Hawaii
- **Current address of PI**: Department of Chemistry, Lehigh University, 6 E. Packer Ave., Bethlehem, PA 18015.
- **Total grant period**: 08/01/07 – 07/31/12. $725,000
- **DOE/Office of Science Program Office**: Basic Energy Sciences
- **DOE/Office of Science Program Office Technical Contact:** Raul Miranda

Studies Performed in Stage I of Grant (8/1/07 – 12/31/08).

In the early stages of this DOE-funded research project, we sought to prepare and study a well-defined nickel-alkyl complex containing tridentate nitrogen donor ligands after Fu had published his initial report showing that pybox ligands could successfully catalyze alkyl-alkyl cross-coupling reactions.[1] We found that reaction of (TMEDA)$NiMe_2$ (**1**) with terpyridine ligand cleanly led to the formation of (terpyridyl)NiMe (**2**, eq 4), which we also determined to be an active alkylation catalyst (see below).[2-4] The thermal stability of **2** was unlike that seen for any of the active pybox ligands, and enabled a number of key studies on alkyl transfer reactions to be performed,[2-4] providing new insights into the mechanism of nickel-mediated alkyl-alkyl cross-coupling reactions. For instance, we showed that **2** can effectively transfer its methyl group to alkyl iodides affording cross-coupled alkanes in high yields, as exemplified in eq 5 (tpy'= 4,4',4"-tri-*tert*-butyl-terpyridine). Surprisingly however, the closely related Ni(II)-alkyl halide complex **3** did not react with excess transmetalating agent to afford the same product (eq 6). This result argued against a two-electron mechanism in a catalytic cycle by which a (terpyridyl)Ni(0) fragment oxidatively adds an alkyl halide to produce **3** and subsequently undergoes a simple transmetalation reaction to afford cross-coupled product. In addition to the mechanistic studies, we showed that the terpyridyl nickel compounds can catalytically cross-couple alkyl iodides in yields up to 98% and bromides in yields up to 46 %.[3] The yields for the bromides can be increased up to 67 % when the new palladium catalyst [(tpy')Pd-Ph]I is used.[5]

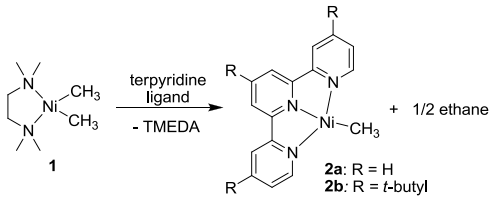

(4)

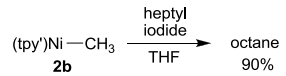

(5)

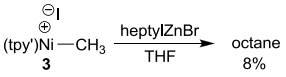

(6)

Since our development of the above terpyridyl nickel system, recent reports (which are also based on DOE-funded research) have also shown that it can be used to stereoselectively prepare *C*-alkyl glycosides.[6,7]

Magnetic and computational studies on (terpyridyl)NiMe. Notably, the overall reaction described in eq 4 also proceeds with a net reduction of the organometallic species. The unique structure and stability of **2**, as well as its central role in cross-coupling catalysis, warranted further studies of this paramagnetic organometallic compound. Magnetic and DFT studies were performed[3] to determine the electronic structure of **2** in order to lay the groundwork for future studies that aim to correlate trends between the *electronic* structures of catalysts with activities. If such a trend exists, then one may be able to rationally optimize future catalysts to ultimately increase the efficiency and scope of the cross-coupling reaction. A reduction of **1** to an odd-electron species was confirmed by EPR spectroscopy, and complex **2a** provides a strong unresolved EPR signal with isotropic $g = 2.021 \pm 0.002$ at room temperature in THF solution. Interestingly, the *g* values suggest a more organic based radical, rather than a metal-centered one, implying that the charge-transfer state consisting of a Ni(II)-methyl cation and a reduced ligand (Chart 1) is the ground-state structure. The unusual electronic structure of **2** suggested by the EPR data can have large implications for cross-coupling catalysis, as activities may correlate with the ability of the tridentate ligands to stabilize a radical anion. To further expound this intriguing EPR result, DFT calculations (unrestricted B3LYP/m6-31G*) were performed[3] on **2a** in order to determine the spatial distribution of the spin density. Geometry optimization yielded a planar (except for the methyl hydrogens), approximately square complex, the geometry of which agrees well with the X-ray crystal structure. A number of population analyses were also included in the DFT calculations, and all show that the majority of the spin density in **2a** resides on the terpyridine ligand. An isodensity representation of the SOMO of **2a**, depicted in Figure 1a, also shows that the unpaired electron is delocalized over the aromatic ligand. The spin density calculations in the planar conformation are thus in full agreement with the EPR data and support a ground state structure that is most properly described as a nickel(II)-alkyl cation bearing a reduced terpyridine ligand.

Chart 1

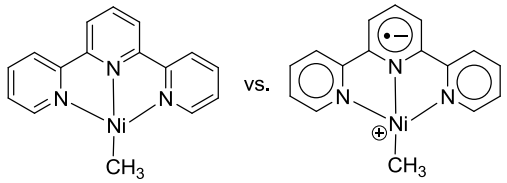

We have also determined optimized geometries and energies of **2a**, constraining the N_2-Ni-C bond angle to five values between 180° and 120°, in order to explore the effect of the catalyst geometry on the electronic structure.[3] Figure 1b shows that the N_2-Ni-C angle can bend about 15° without raising the energy more than 1 kcal/mol. However, substantial bends require 10-15 kcal/mol. DFT calculations at these strongly bent geometries predict that the spin density on the nickel increases relative to the planar form. This additional insight provided by the DFT studies suggests that ligands that effect the positioning of the pendant alkyl group relative to the plane of the other three nitrogen atoms can thus, in theory, modulate this charge transfer chemistry by allowing or not allowing optimum overlap of the d_{yz} orbital with the nitrogen of the central pyridyl ring of the ligand as represented in the SOMO (Figure 1a).

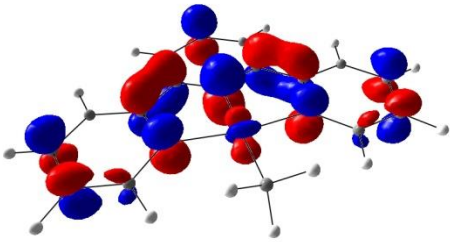

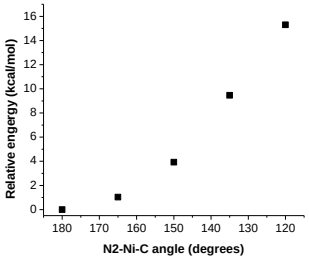

Figure 1a (left): Singly occupied molecular orbital of complex **2a** from unrestricted DFT calculations. **Figure 1b** (right) Optimized relative energies of (tpy)NiMe as a function of the constrained N_2-Ni-C(Me) angle.

Since the report of the above magnetic and computational studies for this Final Report, two other theoretical examinations of the alkyl-alkyl cross-coupling reactions have appeared which focused heavily on our initial findings.[8,9]

Using the Redox Active Ligands in Cross-Coupling Catalysis. Catalysis was observed, and based on our studies for this Final Report,[3] an updated mechanism for the nickel-catalyzed alkyl-alkyl Negishi reactions is proposed in Scheme 2. This mechanism involves reaction of a (terpyridyl)Ni(alkyl) complex such as **4** with an alkyl halide to form **5** and alkyl radical. The redox potentials of **2a** and **2b** were found to be -1.32 and -1.44 V (vs Ag/Ag^+ in THF solution), making the alkyl halide reduction by **2** thermodynamically favorable. This one electron, ligand-based redox event may provide some insight into how stereo-convergence might be possible for the asymmetric versions of this reaction using chiral ligands like pybox. We speculate that alkyl halide reduction by the ligand leaves an alkyl radical in close proximity to the metal center, where an oxidative radical addition ensues to afford the nickel(III)-dialkyl species **6**. If L is therefore chiral, enantioselective addition of the radical to nickel may take place. Fast reductive elimination of cross-coupled alkane then occurs to release electrons from the antibonding orbital of **6** leaving **7** as the final nickel-containing product of a catalytic cycle. We have already shown that indeed (tpy')NiI is a viable catalyst for alkyl-alkyl Negishi reactions.[3] With regard to the electronic structures of the proposed intermediates, we can say that spin-unrestricted DFT analyses of **6** and **7** predict that these compounds should be formulated as Ni(III) and Ni(I) complexes, respectively. The oxidation states may also be dictated by the nature of the diimine ligand, as we found that bidentate

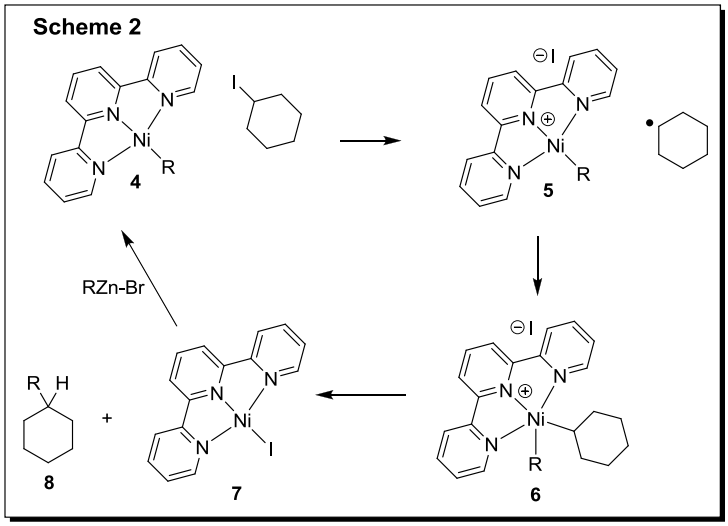

ligands such as bathophenathroline have much different electronic characteristics than the terpyridyl-based counterparts.

Ligand Effects in Alkyl-Alkyl Cross-Coupling Catalysis. To complement the EPR and DFT studies, comparative cross-coupling reactions were performed with the ligands shown in Chart 2. We chose iodo- and bromo-propylbenzene as our alkyl electrophiles, and *n*-pentylzinc bromide as our alkyl nucleophile (Table 1). Table 1 lists all of the cross-coupling yields obtained for the ligand survey, and a full discussion of the ligand effects has been published during the last grant period.[3]

Chart 2

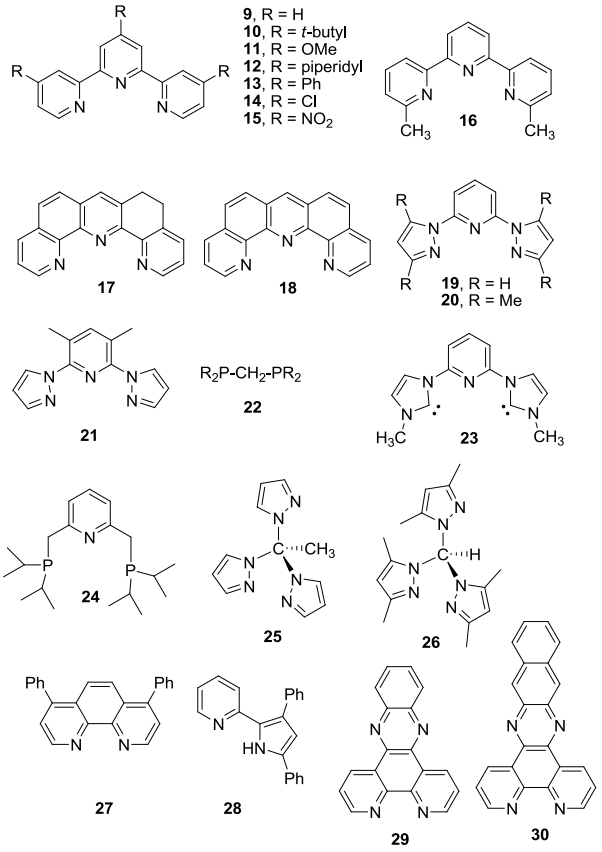

Table 1

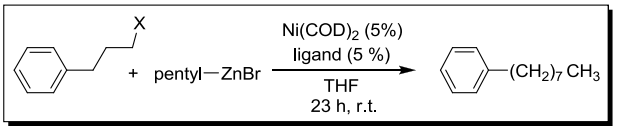

entry	*Ligand*	*% Yield for X = I*	*% Yield for X = Br*
1	**9**	60	17
2	**9**[b]	54	16
3	**10**	98	46
4	**11**	53	44
5	**12**	38	3
6	**13**	54	33
7	**14**	19	3
8	**14**[c]	44	33
9	**15**	0	0
10	**15**[c]	31	17
11	**16**	6	4
12	**17**	63	59
13	**18**	58	37
14	**19**	67	45
15	**20**	13	16
16	**21**[b]	63	31
17	**22**	0	0
18	**23**	4	1
19	**24**	1	0
20	**25**	3 (2[b])	0
21	**26**	5 (8[b])	1
22	**27**	56	43
23	**28**	3	0
24	**29**	40	27
25	**30**	37	23

[b]Catalyst was $LNiI_2$. [c]Catalyst was $LNiCl_2$

Observation of Linear Bridging Hydrides. Although ligand **22** (Table 2, entry 17) did not support any cross-coupling catalysis, we have been able to identify the major byproducts of the Negishi reactions as [(μ-phosphine)$_2$Ni$_2$X$_2$](μ-H). The bridging hydrides in these derivatives were found to have fundamentally important structures, as some of

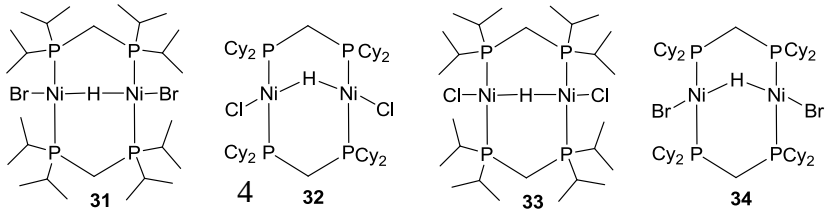

them exhibited linear M-H-M bonding,[10,11] a geometry never before verified for dinuclear metal complexes in the solid-state. It was long believed that the M-H-M linkage in a bridging hydride complex was inherently bent because the bend allows the orbitals of the two supporting metals to be closer in space and potentially interact in a stabilizing fashion.[12,13] The result of a productive interaction is a bonding situation akin to the three-center-two electron bonds in diborane. For this Final Report, we have obtained the solid-state structures of derivatives **31**-**34**,[10] including the neutron diffraction analysis of **33** (in collaboration with Art Schultz at Argonne National Lab).

Complex 31	*Complex 32*	*Complex 33*	*Complex 34*
		Intraatomic	
2.850(15) Br1	2.858 Cl	2.705(11) Cl1	2.905 Br
3.042(14) Br1		2.734(14) Cl1	2.999 Br
2.789(14) Br1		2.642(14) Cl1	3.020 Br
2.743(13) Br1		2.866(14) Cl1	
3.003(16) Br1		2.739(13) Cl2	
2.688(14) Br2		2.798(13) Cl2	
2.908(15) Br2		2.726(12) Cl2	
2.715(13) Br2		2.948(14) Cl2	
2.766(15) Br2			
		Interatomic	
2.769(13) Br1		2.748(10) Cl1	3.040 Br
2.915(14) Br1		2.858(12) Cl1	
2.841(14) Br2		2.709(13) Cl1	
2.729(13) Br2		2.745(11) Cl2	
2.770(15) Br2		2.931(14) Cl2	

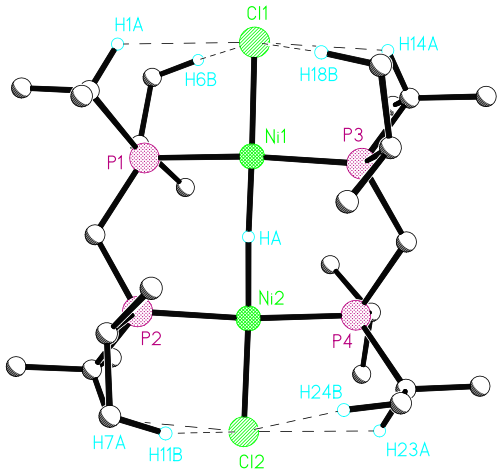

Table 2 (left). Distances of CH-X contacts (Å) shorter than the sum of the van der Waals radii (H,Cl = 2.95 Å, H,Br = 3.05 Å). **Figure 2 (right):** Ball and stick diagram of **33** showing the internal hydrogen bonding interactions between the alkylphosphine and halide ligands. All hydrogens except the bridging hydrides and those involved in hydrogen bonding have been omitted for clarity.

One of the most interesting features of the dimers is that the isopropyl derivatives display linear M-H-M geometries and also exhibit shorter and more numerous CH-to-halide hydrogen contacts than the cyclohexyl counterparts (Table 2), which are bent. Compound **32**, for instance, contains only one internal hydrogen bond and no interatomic contacts per chloride. The isopropyl derivative **33**, on the other hand, exhibited four much shorter internal contacts (Figure 2) and a total of five interatomic contacts per dimer. It thus appears more and more likely that external influences such as sterics, hydrogen bonding, and crystal packing forces largely determine the geometry of the M-H-M bond angle, and that bridging hydrides need not inherently possess a *closed* three-center bond containing stabilizing metal-metal interactions. In fact, Macchi and co-workers have recently shown by high resolution X-ray diffraction that the classically bent $[Cr_2(\mu\text{-}H)(CO)_{10}]$ anion indeed does not show metal-metal orbital overlap in the electron density maps and that the optimized geometry by DFT methods was a linear bridging hydride like the ones that we have observed experimentally.[14]

Mild, Efficient, and Reliable Trifluoromethylations at Copper: Parallel to the alkylation studies with nickel, we explored new methods to manipulate fluoroalkanes since catalytic coupling protocols are desperately needed. Copper has by far shown the most promise in

metal-mediated trifluoromethylation reactions. However, many copper reactions have been plagued by unreliability, the need to use extremely high temperatures, toxic or expensive sources of the CF_3 group, and competing Ullmann coupling and reduction of aryl halides that generally provide lower yields of fluorinated product. Most of the copper couplings reported to date also involved the generation of "Cu-CF_3" *in situ*, making it more difficult to understand and control what was happening at the copper center. We therefore sought for this past grant period to prepare a well-defined Cu^I-CF_3 complex in order to systematically study its reactivity with organic halides. We found the procedure outlined in eq 7 to be the most successful synthetic approach to a stable Cu^I-CF_3 complex. Surprisingly when CF_3-$SiMe_3$ was added to the known NHC copper complex **35**, not only was the desired CF_3 group attached to copper (^{19}F NMR, C_6D_6, δ -33.7) but the trimethylsilyl group was also incorporated into the major product. (A ~80:20 ratio of **36** to the unsilylated (IPr)Cu-CF_3 was observed by NMR spectroscopy). Complex **36** was the first example of an isolable copper(I)-trifluoromethyl complex, and we have communicated the details of its structure and reactivity.[15] Only NMR evidence for solvated Cu^I-CF_3 at -50 ˚C was reported before these above studies,[16] and decomposition was generally observed at higher temperatures. Importantly, others have also noted that the thermal instability and nature of the decomposition products demonstrate that solvated Cu^I-CF_3 is more complex (in terms of aggregation) than previously appreciated, and that control of nuclearity can have significant consequences in the ability to control fluoroalkylations.[16] We have found that the steric bulk of the carbene ligand in **36** rigorously controls the nuclearity, even in solution, as no evidence of dimers or higher aggregates are observed by NMR spectroscopy.

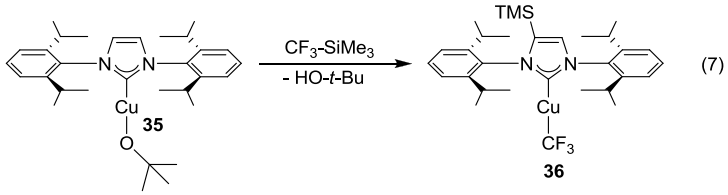

(7)

Reaction of **36** with Ph-I (neat) at room temperature for 44h led to Ph-CF_3 in 33 % yield based on copper. Upon heating, product formation is competitive with decomposition to a brown solid and the formation of an LCu-CF_2CF_3 species and Me_3Si-F as detected by ^{19}F NMR spectroscopy. The presence of Me_3Si-F as a decomposition product in the reaction of **36** with aryl halides suggests that the silylated carbene ring is undesirable in trifluoromethylation reactions. With that in mind, we targeted the use of carbene ligands containing a saturated backbone, like SI*i*Pr shown in complex **37** (eq 8). The SI*i*Pr ligand also has the feature of being less sterically demanding than SIPr, which is desired to facilitate interactions with organic halides. Evidence of greater accessibility to the copper center with the SI*i*Pr ligand is seen by the fact that **37** exists as a dimer in the solid state (as verified by X-ray), whereas **36** is monomeric. Complex **37** can be converted to the extremely air-sensitive **38** (^{19}F NMR (C_6D_6) δ -33.1) upon treatment with CF_3-$SiMe_3$ with no evidence of TMS incorporation into the carbene ring.

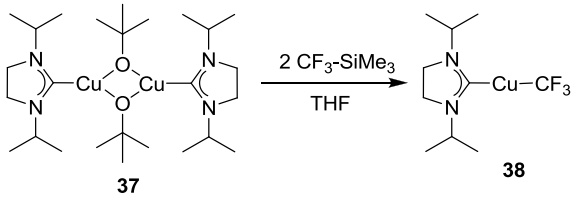

(8)

We were pleased to see that complex **37** serves as an efficient precatalyst for trifluoromethylations of aryl halides. In a test screen, reaction of **37** and TMS-CF_3 in neat iodobenzene at room temperature led to Ph-CF_3 in 84 % yield based on copper. Under similar conditions, the use of complex **38** without any added TMS-CF_3 also led to Ph-CF_3, but in slightly lower yields (67 %) due to competing formation of Cu-CF_2CF_3 side products as detected by ^{19}F NMR spectroscopy. The efficiency of the trifluoromethylation reactions can be greatly enhanced by the use of DMF solvent. Table 3 shows that yields of trifluoromethylated products for a variety of organic halides are consistently in the 90% range. The state-of-the-art methods prior to these reports have used TMS-CF_3/Cu-I/KF with the absence of ligands at copper, either at room temperature or at 80 ˚C. For comparison, runs employing the TMS-CF_3/Cu-I/KF system were performed under the same conditions as our runs using complex **37** as a catalyst precursor, and the results are provided in Table 3. Not only are the yields higher with the well-defined SI*i*Pr ligand, but they are also consistent for a variety of aryl idodides. Note that in some cases the yield of product by our protocol is nearly four times higher!

Table 3. Trifluoromethylations mediated by **37** in DMF solvent compared to yields using Cu-I and KF in place of **37**. Yields were recorded after 112 h and measured by ^{19}F NMR relative to 1,3-dimethyl-2-fluorobenzene as an internal standard. Yields based on copper as the limiting reagent.

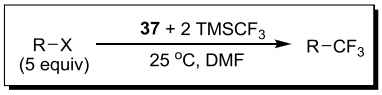

Entry	*Starting material*	*Product*	*Yields (%)*	*Yields using the Cu-I, KF protocol*
1		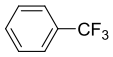	**94**	25
2	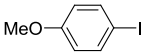	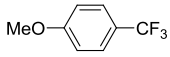	**91**	62
3	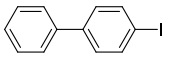	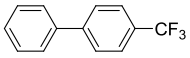	**99**	41
4		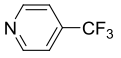	**99**	70
5		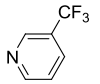	**94**	3[a]
6	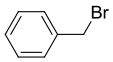	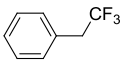	**58**	29

[a]: a white precipitate was observed

Catalytic conditions using one equivalent of KO*t*-Bu to regenerate the $[(NHC)Cu(Ot\text{-}Bu)]_2$ complex were ineffective; as KO*t*-Bu reacts with TMS-CF_3 at a background rate which is too fast (CF_3H was determined to be the main product under catalytic conditions). If a nucleophile can be developed to preferentially transmetalate copper into a species that reacts with TMS-CF_3, then catalysis may be possible at copper. Planned studies to develop more compatible nucleophiles are herein proposed.

Copper-catalyzed decarboxylation of trifluoroacetate: Perhaps the most intriguing way reported to date to prepare an activated copper reagent for fluoroalkylations involves the use of inexpensive and readily available perfluoroacetate ions. Chang has found that treatment of Cu(I) salts with sodium trifluoroacetate at elevated temperatures leads to a decarboxylation reaction to afford the requisite "Cu-CF_3" for further reactions with limited organic substrates (eqs 9 and 10). [17-22] The significance of these results is that not only is trifluoroacetic acid much cheaper than Me_3Si-CF_3 (and most other environmentally benign sources of CF_3),[23] but also that many perfluoroalkylcarboxylate derivatives can easily be made by electrolysis of parent carboxylic acid in fluoride solutions.[24] The PI is unaware of a better methodology to make longer chain fluoroalkyl nucleophiles. The obvious drawback for this method is the high temperatures involved, and Chang noted that evolution of CO_2 begins at 140 °C.[22]

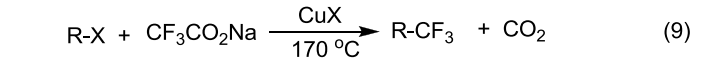

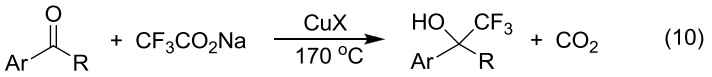

In related work, Gooßen and co-workers reported in *Science* in 2006 the synthesis of biaryls via catalytic decarboxylative cross-coupling.[25] The work was impressive as the authors used copper to decarboxylate aryl acetates into aryl copper nucleophiles and palladium to activate aryl electrophiles (Scheme 3). However, the temperatures required were still in excess of 150 °C when catalytic amounts of copper were used.[25] These results were in accordance with Chang's report that the copper mediated decarboxylation of CF_3CO_2Na required extreme temperatures.[22] No perfluoroalkylations were reported.

Scheme 3

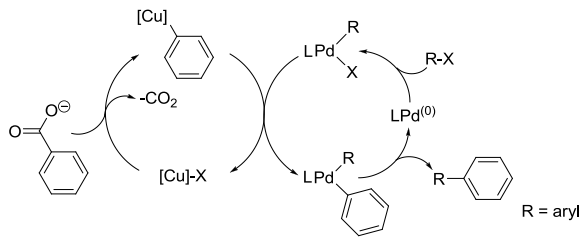

The use of perfluoroalkylcarboxylates as fluorous synthons might also be amenable to nickel chemistry, as Cookson and co-workers reported that diimine complexes of nickel bearing fluorous arylcarboxylates ligands lose CO_2 in refluxing toluene (eq 11).[26] The loss of CO_2 occurred at lower temperature than those in the aforementioned examples with copper, although it is difficult with this limited data to separate out metal effects from substituent (aryl vs alkyl) effects. Nevertheless, this general reactivity in the context of cross-coupling reactions is important, as nickel also has the advantage of being able to cross-couple alkyl[1-4] and aryl[27-30] electrophiles at temperatures typically lower than those seen for copper. This raises the possibility of using a single metal to catalyze perfluoroalkylations. To our knowledge, the reactivity of nickel with perfluoroalkylcarboxylates in this regard has yet to be investigated.

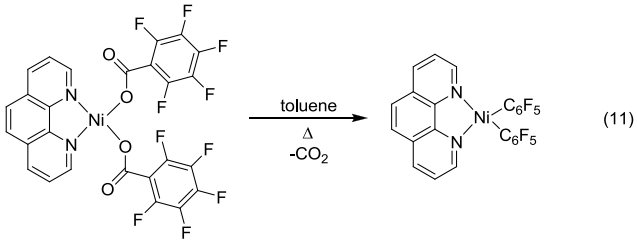

For this Final Report we have been able to prepare and fully characterize (including X-ray) the well-defined trifluoroacetate complex **39** (eq 12) and establish that upon heating, this molecule indeed decarboxylates in the presence of phenyl iodide to afford trifluorotoluene in 56 % yield. With this significant result in hand, we plan to pursue systematic studies on well-defined complexes to understand how to lower the temperatures of decarboxylation and increase product yields.

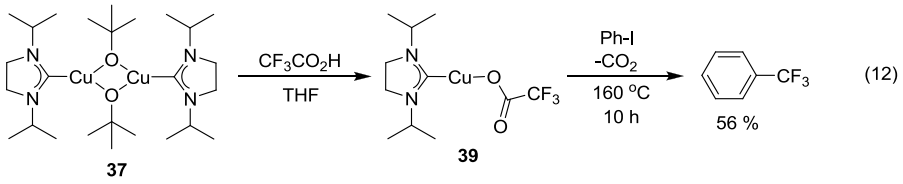

(12)

Nickel Mediated Fluoroalkyl Cross-Couplings: Since the copper trifluoromethylation reactions described above were general for aryl iodides, we targeted other metals which are known to activate the more stubborn R-Br and R-Cl substrates. The use of a nickel catalyst is an attractive alternative to palladium for fluoroalkyl cross-coupling not only for cost reasons, but also for the fact that nickel has demonstrated much more success in alkyl-alkyl cross-coupling reactions. Moreover, having easily accessible multiple oxidation states in nickel raises the intriguing possibility of performing redox triggered reactions like oxidatively induced reductive eliminations (eq 13).[31,32] Such one-electron redox chemistry would be inherently more difficult to perform with palladium. Importantly, these redox-triggered reactions are amenable to catalysis, as we have shown that catalytic alkyl-alkyl cross-coupling reactions involving terpyridine-based nickel catalysts operate by a stepwise redox shuttle out to Ni^{III}. As there have been few reports of any Ni-CF_3 complexes in the literature, the chemical foundations relevant to cross-coupling that functional group needed to be established. During this past Final Report, we began our initial efforts to understand the many factors controlling trifluoromethylations with nickel. We were able to prepare the four new (dippe)Ni(aryl)(Br) complexes **40** – **43** and the four new (dippe)Ni(aryl)(CF_3) complexes **44** – **47** in good isolated yields (Chart 3). However, we found that none of the new (dippe)Ni(aryl)(CF_3) complexes yielded Ar-CF_3 upon heating. Solutions of

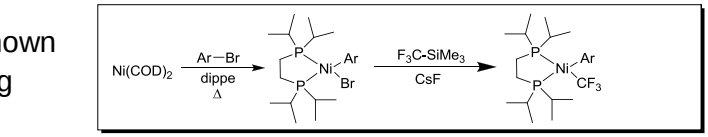

(13)

Chart 3

aryl halide product	*yield* (%)	*aryl CF_3 product*	*yield* (%)
40	65	**44**	57
41	74	**45**	54
42	88	**46**	70
43	80	**47**	68

(dippe)Ni(aryl)(CF_3) are stable in THF solvent for days at room temperature, but eventually turn green and ultimately afford the biaryl and complex **49** (eq 14). This reaction is accelerated in CH_2Cl_2 solvent, where substantial biphenyl production occurs only in hours. We tentatively attribute the common diamagnetic green intermediate (^{19}F NMR (CD_2Cl_2 δ -75.5 (dd, *J* = 41.6, 18.8 Hz)) to the formation of the dinuclear species **48**, containing a nickel-nickel bond. Related nickel(I) dimers are known, and the presence of such an intermediate also nicely explains the formation of (dippe)Ni(CF_3)$_2$ as a major side product in the transmetalation procedure. In contrast to reluctance of **44**-**47** to reductively eliminate Ar-CF_3, their non-fluorinated analogues [(dippe)Ni(Ar)(CH_3)] were found to decompose within minutes at room temperature to afford Ar-CH_3 in near quantitative yields.

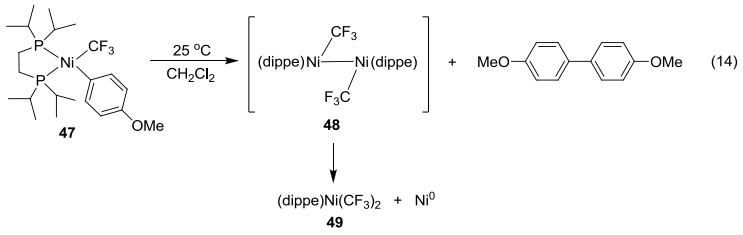

Because thermolysis of the (dippe)Ni(aryl)(CF_3) complexes did not yield any cross-coupled product, we explored the use of additives to facilitate reductive elimination reactions at **44** (Table 4). Two potent oxidants $[Fe(bpy)_3]^{3+}$ and $[(NH_4)_2Ce(NO_3)_6]^{4+}$ did not yield any of the desired trifluorotoluene, even when used in excess (entries 1 and 2). Ar-H was detected as the major organic product in these oxidation reactions. (We have since received a tip that performing the reactions in solvents like 1,2-difluorobenzene in which there are no abstractable protons may help avoid side reactions to form Ar-H). Excess Ph-Br, which would be present in any catalytic trifluoromethylation process involving Ph-Br, did not lead to any products (entry 3), even at elevated temperatures. Zinc reagents were found initiate reductive elimination of Ar-CF_3, but only to a small degree (entries 4 and 5). Surprisingly, the introduction of water had the most beneficial effect, producing the desired product in 22 % yield (entry 6). Although attempts to further optimize the cross-coupling reactions in entries 4 – 6 were fruitless, the data does suggest that trifluoromethylations are indeed possible at nickel, even at room temperature. Ligands of other geometries and coordination number may better coax a reductive elimination of Ar-CF_3 at nickel, and these were the subject of the Proposed Research for the next grant period.

Table 4

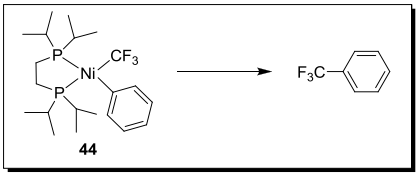

Entry	*Additive*	*Conditions*	*Yield of $PhCF_3$ (%)*[a]
1	$Fe(bpy)_3(PF_6)_3$ 1 equiv	THF, 25 °C 3 days	0
2	$(NH_4)_2Ce(NO_3)_6$ 5 equiv	THF, 25 °C 3 days	0
3	Ph-Br 95 equiv	THF, 25 °C 3 days	0
4	PhZnBr 25 eq	THF, 25 °C 3 days	11
5	$ZnBr_2$ 5 equiv	THF, 25 °C 14 h	19
6	H_2O 100 equiv	toluene, 80 °C 5 h	22

[a] yields determined by ^{19}F NMR relative to 2-fluoro-1,3-dimethylbenzene as an internal standard

Studies Performed in Stage II of Grant (01/01/2009 – 7/31/2012).

Progress with Alkylation Chemistry.

The best route to the targeted [(tpy)NiBr] (**1**) was found to involve the comproportionation reaction of [(dme)$NiBr_2$] and [$Ni(COD)_2$] in the presence of two equivalents of terpyridine. This reaction was driven to high yields of product formation (72 % isolated) by the precipitation of **1** from THF solvent. Complex **1** was found to be a dark green air-sensitive compound which is insoluble in most organic solvents. Crystals can be grown from DMF, however, and the most unique feature of the solid-state structure of **1** is that surprisingly **1** crystallizes in a square-planar geometry. With this geometry in mind, the location of the unpaired electron (Chart 1) became an issue as the vast majority of square-planar nickel complexes consist of nickel in the plus two oxidation state. Since the related compound [(tpy)Ni-CH_3] (**2**) also crystallizes in a square-planar arrangement with an electronic structure that is most appropriately described as [$(tpy^{-1})Ni^{II}$-CH_3],[2] it was tempting to say that the most proper way to describe **1** is the similar form shown to the right of Chart 1. However, the EPR spectroscopy and DFT studies performed for this Final Report suggest that analogies between [(tpy)Ni-CH_3] and **1** based solely on X-ray crystallographic evidence are not appropriate.

Chart 1

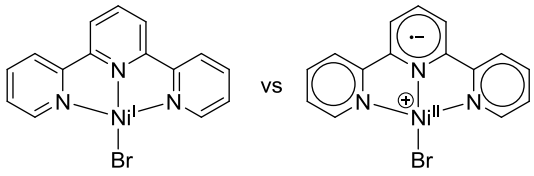

The low-temperature solid-state powder EPR spectrum of **1** exhibits an axial signal with $g_{||}$ = 2.256 and $g\perp$ = 2.091 consistent with a metal-centered $d_{x^2-y^2}$ ground state. In DMF solution, an isotropic signal can be observed with g_{iso} = 2.139. Thus, both in the crystal structure form and in solution, signals for a radical with substantial metal character are observed for **1**. These EPR results are telling in that the electronic structure of **1** is significantly different than [(tpy)Ni-CH_3] (**2**) as the *g*-values of **2** were more indicative of a ligand-centered radical (g_{iso} = 2.021 at room temperature and g_x = 2.056, g_y = 2.021 and g_z = 1.999 at 77K).[2]

DFT calculations were also performed to lend support to the experimental evidence for the Ni(I) formulism for complex **1**. Unrestricted geometry optimizations were performed along with population analyses, and selected results are shown below. The below chart shows that for both [(tpy)Ni-I] and [(tpy)Ni-Br], the majority of the spin density resides on the metal. The location of the spin densities found for [(tpy)Ni-I] and [(tpy)Ni-Br] is in sharp in contrast to that observed for [(tpy)Ni-CH_3], where over 90 % of the spin density was calculated to reside on the ligand.[2]

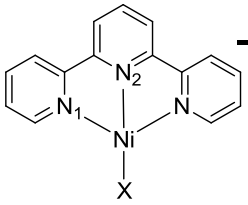

Population Analysis	[(tpy)Ni-CH_3]			[(tpy)Ni-Br]				[(tpy)Ni-I]		
	Ni	N2	N1	Ni	N2	N1	Br	Ni	N2	N1
Lowdin	0.087	0.179	0.059	1.171	-0.001	0.021	0.054	1.022	0.076	0.059
Mulliken	0.076	0.187	0.063	1.180	-0.003	0.014	0.067	1.034	0.076	0.063

Interestingly, the computations show that [(tpy)Ni-Br] refines to a near planar form in the gas phase, while the [(tpy)Ni-I] derivative retains its bent shape (as observed experimentally). A speculation is that the non-planarity of the latter is a consequence of the large size of the iodide ligand. A plot of the SOMO of **1** is shown in Figure 1, and the $d_{x^2-y^2}$ component to the SOMO correlates well with the EPR data. The LUMO of **1** is also shown in Figure 1, along with that of its one-electron oxidized form. These DFT studies match our electrochemical studies (see below) which show that the first two reductions are indeed ligand centered.

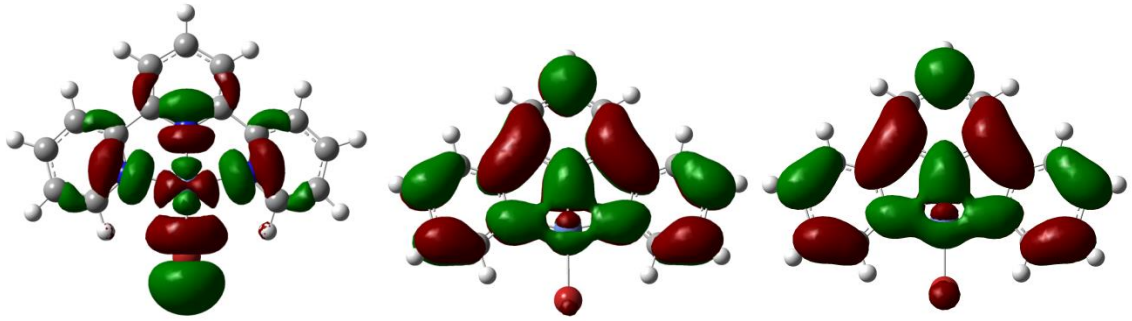

Figure 1: Left: SOMO of complex **1** from unrestricted DFT calculations. Middle: Graphical representation of the LUMO of **1**. Right: Graphical representation of the LUMO of $[(tpy)Ni\text{-}Br]^+$ (singlet form).

The calculated bond lengths also do not show any major disruptions in the aromaticity of the ligand, consistent with a metal-centered SOMO.[14,15] Also of note is the longer nickel-nitrogen bond lengths of **1** compared with [(tpy)Ni-CH_3] (Chart 2), consisted with the antibonding nature of the $d_{x^2-y^2}$ in the SOMO of **1**.

Chart 2. DFT-calculated bond lengths for **1**. Bond lengths in red are those calculated for [(tpy)Ni-CH_3].[2]

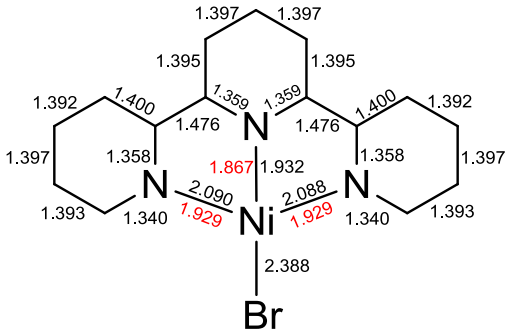

So although the geometries of LNi-Br and LNi-R were quite similar, the electronic and magnetic properties varied substantially. In particular, we showed that the replacement of an organometallic ligand like a methyl group with a simple halide can significantly alter the character of a SOMO in a molecule containing a redox active ligand. The much stronger sigma bonding methyl ligand in [(tpy)Ni-CH_3] evidently raises the $d_{x^2-y^2}$ frontier orbital higher than does the bromide counterpart, making it preferable to put an electron in the terpyridine ligand.

The electrochemistry of **1** was also important to establish in this Progress Report, as we discovered that **1** is an effective electrocatalyst for the fluoroalkylation of olefins (see below). The cyclic voltammogram for **1** reveals that two quasi-reversible reductions occur at -0.76 V and -1.35 vs. Ag/AgCl in DMF solvent. Intriguingly, we found that reductions of the related dibromide [(tpy)$NiBr_2$] occur at the same potentials. To probe the solution redox chemistry further, exhaustive titrations were performed to fully characterize important redox species that may be present in solution. The details have been published, and the bottom-line result of these titrations is that the overall ligand sphere (one vs. two coordinated terpyridine ligands) plays more of a role in determining the redox potentials of these derivatives than do the formal oxidation states of the nickel ions in the solution phase. These results stem from the fact that the first two reductions of terpyridine-ligated nickel complexes described above are ligand-centered reductions and are to a large extent independent of the oxidation state of the metal. The syntheses, magnetism, and computational and electrochemical studies of [(tpy)Ni-Br] and derivatives has been recently published in *Inorg. Chem*.[33]

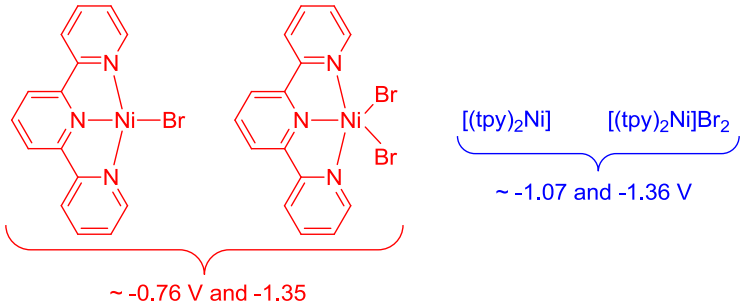

b) Redox Properties of Metal-Alkyl versus Metal-Perfluoroalkyl Complexes.

To segue from the alkylation to the perfluoroalkylation chemistry, we sought to understand the degree to which the trifluoromethyl ligand affects one-electron redox events at first-row metals. We felt this was important as first-row transition metals often react with organic halides via radical-based mechanisms involving one-electron changes in metal oxidation states. We were surprised to discover that there was not a single report on the electrochemical properties of nickel- or copper-trifluoromethyl complexes. For this Progress Report, we performed a simple comparison of the redox properties of nickel and copper organometallic and perfluoro-organometallic complexes to fill the gap in knowledge at the time. The results are summarized in Chart 3. This work on the fundamental redox properties of these compounds, published in *Organometallics*, had been listed as a top-five "Most Read" (most downloaded) paper for the month.[34] One of the more striking aspects of Chart 3 is the incredibly large difference in oxidation potentials for the metal-methyl complexes versus the metal-trifluoromethyl counterparts. In fact, in some cases (complex **5**, for example), the presence of a CF_3 group raises the redox potential to a point where there are few practical chemical oxidants capable of

oxidizing the complex by an outer-sphere electron transfer mechanism (all potentials are the first oxidation potential versus the Fc/Fc+ couple).[35] However, ligand effects are important. Complexes **12** and **13**, for instance, do not show any substantial differences in the oxidation potentials due to the fact that the HOMOs for these compounds are localized on the central nitrogen atom of the ligand. Since oxidations are taking place on the pincer ligand, the potentials are minimally influenced by the nature of the other supporting ligands (C_2F_5 vs Cl).

Chart 3

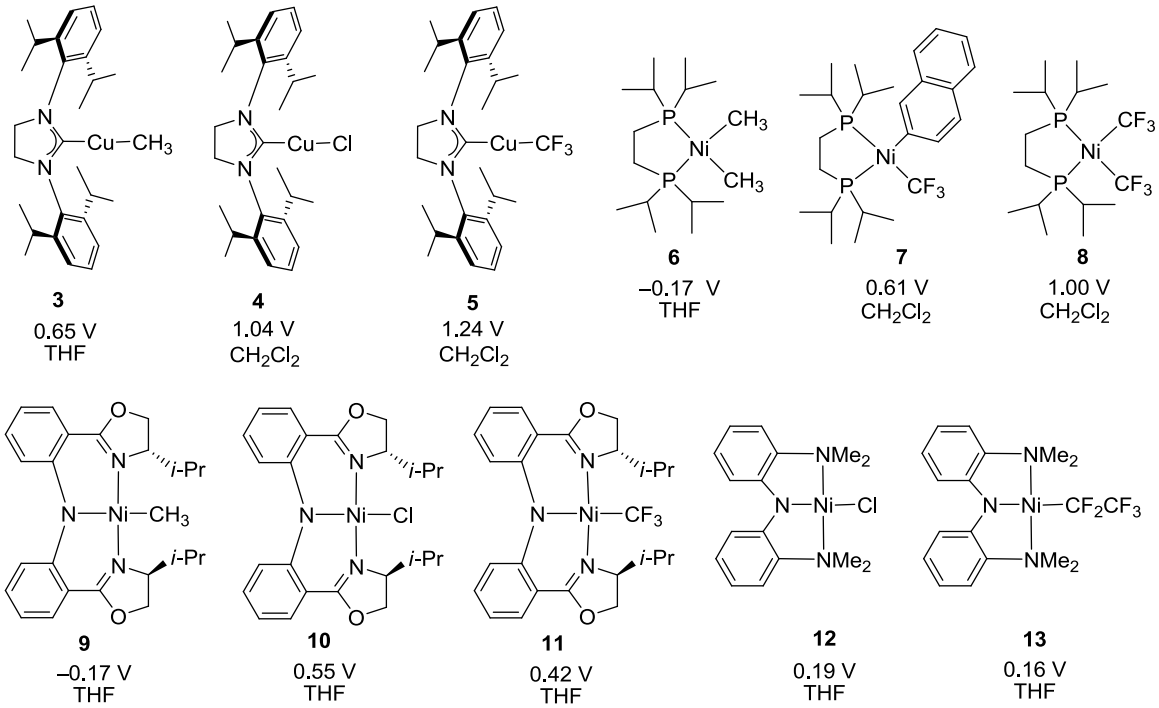

3 0.65 V THF

4 1.04 V CH_2Cl_2

5 1.24 V CH_2Cl_2

6 –0.17 V THF

7 0.61 V CH_2Cl_2

8 1.00 V CH_2Cl_2

9 –0.17 V THF

10 0.55 V THF

11 0.42 V THF

12 0.19 V THF

13 0.16 V THF

Progress with Perfluoroalkylation Chemistry

a) Fundamental studies of bipyridine nickel perfluoroalkyl complexes. Nickel bipyridine complexes have played a significant role in synthetic chemistry. Much of the fundamental information regarding reductive elimination processes,[36-45] redox events,[39,42,46-49] insertion reactions,[50-63] polymer synthesis,[64-75] and electrocatalytic couplings[76-80] using nickel comes from studies initiated with complexes bearing the bipyridine ligand. For this Progress Report, we became interested in preparing nickel bipyridine complexes bearing two perfluoroalkyl ligands in order to compare and contrast the reactivity with that known for bipyridine nickel dialkyl complexes. The only two known fluoroalkyl complexes of a nickel bipyridine framework, however, were metallacycles that were both prepared by oxidative cyclization of fluorinated olefins.[81-83] There were no reports on the preparation of linear fluoroalkyl complexes based on nickel bipyridine, and these are the type of complexes that are needed to study processes most relevant to synthetic applications, like reductive elimination.

Another motivation for preparing bipyridine nickel bis-perfluoroalkyl complexes is that they may offer an internal spectroscopic handle to further study the electronic properties of perfluoroalkyl ligands. Square planar nickel complexes of 2,2'-bipyridine (or derivatives) show intense metal-to-ligand charge transfer bands in the visible part of the electronic absorption spectra. A detailed study of the UV-Vis spectra of the closely related complexes [(bpy)Ni(CH_3)$_2$] (**14**), [(bpy)Ni(Mes)$_2$] (**15**), and [(bpy)Ni(Mes)Br] (**16**) (Mes = mesityl = 2,4,6-trimethylphenyl) has recently been reported,[84] and while the low energy transitions responsible for the long-wavelength absorption of **15** and **16** have distinct contributions from the aryl co-ligand, the [(bpy)Ni(CH_3)$_2$] complex exhibited almost pure metal(d)-to-ligand(π*) charge-transfer transitions. With this in mind, we were quite interested to see how the optical spectrum would change upon fluorination of the alkyl co-ligands, as changes would directly reflect the electronic properties of the metal and fluoroalkyl groups. In order to assess how fluorination of the organic co-ligands affects the bipyridine nickel system, we prepared [(dtbpy)Ni(CF_3)$_2$] (**17**), [(dtbpy)Ni(CF_2CF_3)$_2$] (**18**), and [(dtbpy)Ni(CH_3)$_2$] (**19**) (dtbpy = 4,4'-di(tert-butyl)-2,2'-bipyridine). **17** and **18** were successfully prepared by the route shown in eq 16. A striking feature of the molecular geometries of **17** and **18** is the large distortion from square planarity. Figure 2 shows views along the N1-Ni-N2 planes of all structures that were isolated. The *trans* nitrogen-nickel-carbon bond angles in **17** were found to be 159.7(2) and 165.1(2)°, far from the idealized 180°, and those for **18** showed an even larger distortion at 152.2(2)°. Steric interactions of the fluorines with the 6 and 6' hydrogens of the bipyridine ligand are most likely responsible for this distortion as the nickel center bearing the perfluoroethyl groups in **20** adopted a far less-distorted square-planar arrangement (Figure 2). Despite the distorted geometries, complexes **17** and **18** are thermally stable (unlike the dimethyl derivative which loses ethane upon gentle warming) and can be exposed to air for weeks without noticeable decomposition. The non-fluorinated dimethyl analogue is extremely air-sensitive.

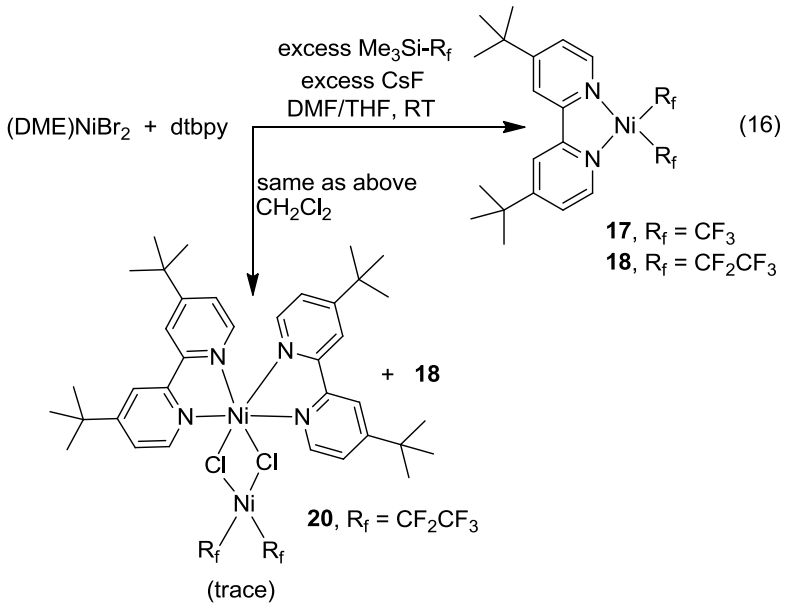

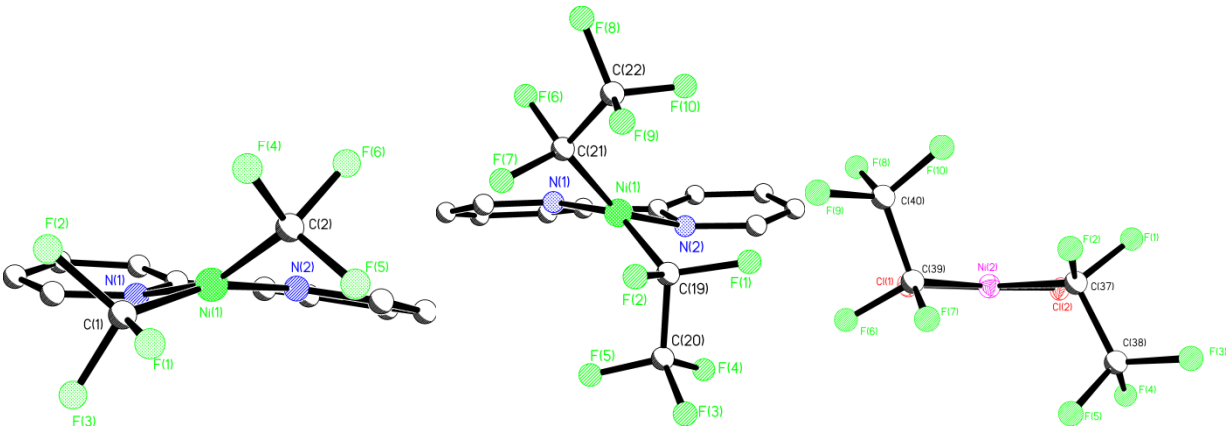

Figure 2. Solid state structures of **17** (left), **18** (middle), and **20** (right). *t*-Butyl groups and all hydrogens removed for clarity. Only the immediate coordination around Ni2 is shown for **20**.

The colors of the new metal complexes deserve mention. Crystals and solutions of **17** are yellow and those of **18** are orange, whereas that of the non-fluorinated [(dtbpy)Ni(CH_3)$_2$] **(19)** derivative is dark green (similar to the known [(bpy)Ni(CH_3)$_2$]).[85] The experimental visible spectra are shown to the right. The bis-CH_3 derivative shows two intense and broad absorption bands at 402 nm and 640 nm.

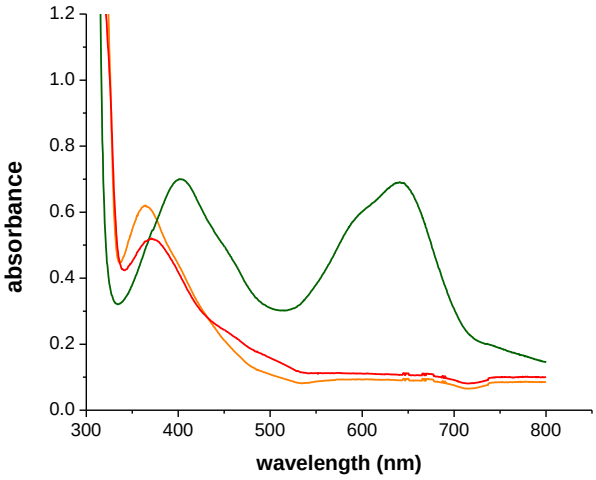

Deconvolution of the known [(bpy)Ni(CH_3)$_2$] spectrum by time-dependent DFT (TD-DFT) showed that these low energy transitions are purely MLCT in character.[84] The most striking feature of the spectra of the bis-perfluoroalkyl complexes is that the low energy absorption bands from 600-700 nm for the bis-perfluoroalkyl complexes **17** and **18** were found to be suppressed, but the band centered ~370 nm was still present. The likely explanation is that the corresponding transitions for these bands are of very mixed character, including contributions from the Ni–CF_3 sigma bonds. Thus, while a general view on the absorption spectra would suggest similar transitions for both the CF_3 and CH_3 complex with a marked blue-shift for the CF_3 derivative and a dramatic loss of intensity for the low-energy charge transfer absorption, a closer look reveals that only the high-energy $\pi \rightarrow \pi^*$ transitions are of similar character, while the long-wavelength charge transfer absorptions differ largely in character, when replacing CH_3 by CF_3. The main differences seem to arise from the involvement of orbitals with CF_3 contributions (or Ni–CF_3) for [(bpy)Ni(CF_3)$_2$] while the CH_3 coligand does not contribute to the transitions of [(bpy)Ni(CH_3)$_2$]. Another possible explanation for the absence of a low energy band is that strong geometric distortions are disabling efficient Ni(3d)-bpy(π^*) overlap. A full TD-DFT analysis of the molecular orbital contributions to the absorption energies of the bis-perfluoroalkyl complexes is needed to thoroughly understand and describe the electronic spectra, and these studies are currently in progress.

An analysis of the charge distribution in these new complexes was also performed, and Figure 3 shows that fluorination has the known effect of decreasing the charge on the atom attached to the fluoroalkane (namely, nickel). Fluorination also has the effect of dramatically "redistributing" the charge in the molecules. For instance, in the bis-CH_3 complex, the carbon atoms of the methyl group are negatively charged whereas in the bis-perfluoroalkyl complexes the carbon atoms bound to the metal are positively charged with the negative charge residing primarily on the fluorine atoms.

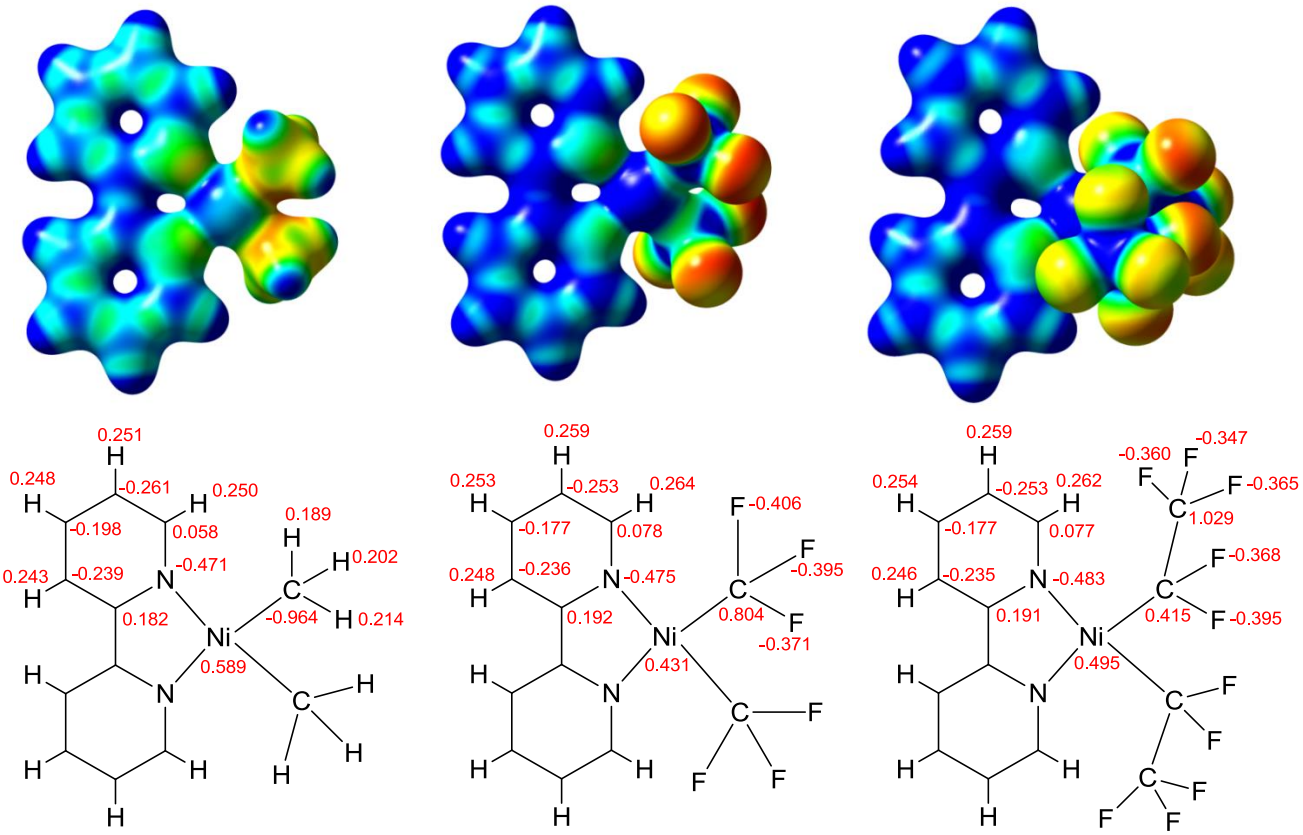

Figure 3. Top, DFT-calculated electrostatic surface potentials of complexes [(bpy)Ni(CH_3)$_2$], [(bpy)Ni(CF_3)$_2$], and [(bpy)Ni(CF_2CF_3)$_2$]. Red indicated regions of negative charge while blue indicates regions of positive charge. Isovalue = 0.02, Density = 0.04. Bottom, calculated atomic charge distributions from a Natural Bond Order analysis.

The nickel center in [(bpy)Ni(CH_3)$_2$] has a calculated charge of 0.589, higher than that of [(bpy)Ni(CF_3)$_2$] at 0.431. Interesting, preliminary calculations suggest that despite the more negative charge on the nickel in the bis-CF_3 derivative, its MLCT is higher in energy than the bis-CH_3 derivative. A comparison of the calculated molecular orbital energies of the two complexes also offers a rationale for the optical behavior. Figure 4 reveals that both the HOMO and the LUMO of the bis-CF_3 complex are largely stabilized over the corresponding orbitals of the bis-CH_3 derivative. However, because the stabilization of the HOMO for the bis-CF_3 derivative is over two times larger than the stabilization of the LUMO, charge transfer transitions for the bis-CF_3 derivative are expected to lie higher in energy. Precedence for significant stabilization of the HOMO by fluoroalkyl groups comes from photoelectron and computational

studies by Puddephatt and co-workers, who showed that the d-orbitals of [(COD)Pt(CF_3)$_2$] were all stabilized relative to [(COD)Pt(CH_3)$_2$].[86] The HOMO stabilization also explains the observed electrochemical features in these new complexes. The bis-CF_3 complex **17** was found to exhibit one quasi-reversible oxidation with an oxidation peak potential at +0.90 V vs Fc^+/Fc in THF solution. Complex **17** is far more difficult to oxidize than the bis-CH_3 derivative **19**, which exhibits an irreversible oxidation at -0.60 V vs Fc^+/Fc in THF solution. This ΔE_{ox} of 1.5 V is the largest we have thus far observed experimentally with nickel.[34] These fundamental studies on the nickel bipyridine system have recently been submitted to *Organometallics*.

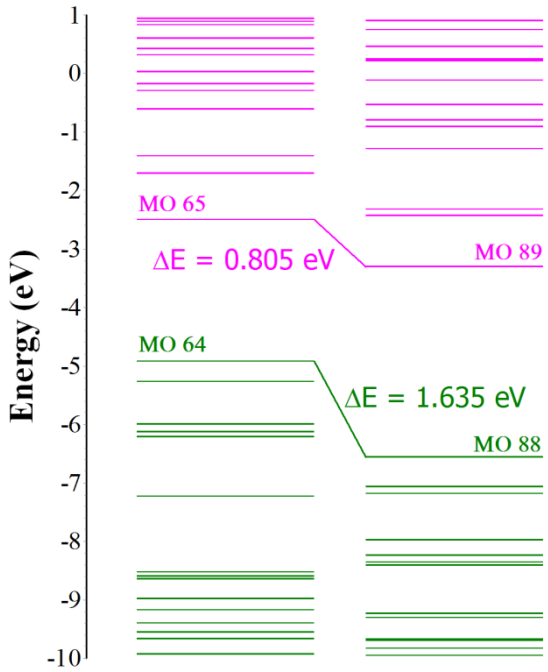

Figure 4 (right). Calculated molecular orbital energy levels in the energy range -10.0 to 1.00 eV showing occupied (green) and unoccupied (pink) MOs of [(bpy)Ni(CF_3)$_2$] (right) and [(bpy)Ni(CH_3)$_2$] (left).

b) Catalytic formation of perfluoroalkylthioethers. It was important to establish some of the basic science behind the nickel bipyridine system as described above, as we also discovered that this metal/ligand combination is effective for the catalytic synthesis of aryl trifluoromethyl sulfides. The previous state-of-the-art method of incorporating an SCF_3 group into unactivated or electron rich aryl halides is outlined in eq 17. Buchwald recently found that a wide range of aryl bromides could be converted into aryl trifluoromethyl sulfides through a palladium catalyzed process employing the hindered BrettPhos ligand.[87] While this method leads to high yields of aryl trifluoromethyl sulfides from aryl iodides and bromides, the combined use of an expensive ligand, an expensive palladium salt, a quaternary amine additive, and stoichiometric use of an expensive silver SCF_3 derivative makes such a reaction unattractive for large scale commercial use. We found that inexpensive nickel bipyridine complexes can be used in conjunction with the cheaper and more convenient [NMe_4][SCF_3] to carry out the same reaction. The [$AgSCF_3$] reagent used in the Buchwald example is actually prepared from [NMe_4][SCF_3], so we have been able to eliminate the need to use silver salts altogether. Yields using Ni(COD)$_2$ and the 4,4'-dimethoxybipyridine (dmbpy) ligand are shown in Table 1. These results have recently been communicated in *JACS*.[88]

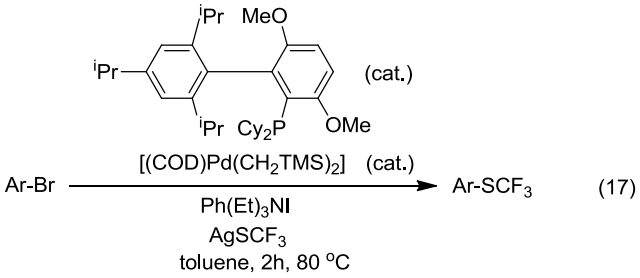

(17)

Table 1. Nickel-catalyzed trifluoromethylthiolation of aryl halides. The yields of $ArSCF_3$ were determined by ^{19}F NMR spectra using trifluoromethylbenzene as internal standard. Isolated yields in parentheses.

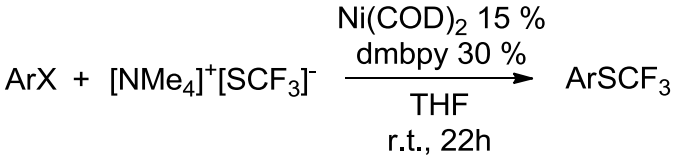

Entry	ArX	Ar-SCF_3	% Yield
1	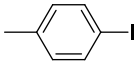	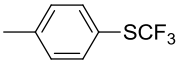	90
2	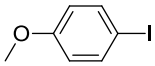	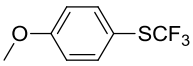	90 (89)
3	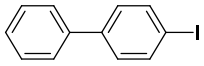	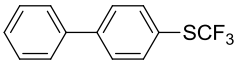	92 (92)
4	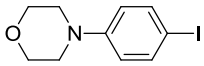	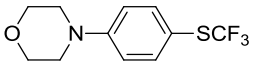	91 (88)
5	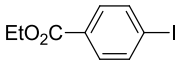	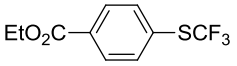	45
6	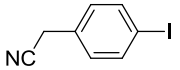	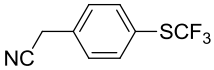	47
7	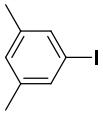	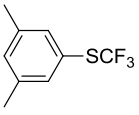	83 (77)
8	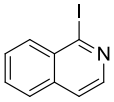		55
9	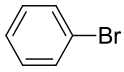	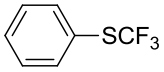	65
11	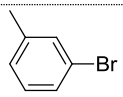	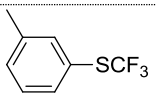	37
12	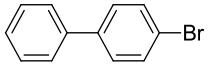	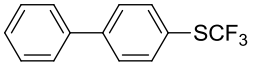	64
13	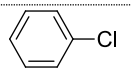	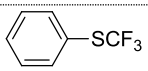	0

c) Decarboxylative trifluoromethylations. Trifluoroacetic acid is theoretically one of the most convenient, inexpensive, and readily available source of the trifluoromethyl group in metal-catalyzed reactions. Moreover, it is known that copper-salts can catalyze the decarboxylation of tridluoroacetate, albeit at temperatures above 150 °C. No one has addressed how ligands might modulate these decarboxylation reactions, so we initiated baseline studies to lay the groundwork for developing new metal-based *catalytic* decarboxylations at lower temperatures. For this Progress Report we have prepared complexes **21** – **23** (Scheme 3), which are based on our [(NHC)Cu-CF_3] complexes that are known to trifluoromethylate organic halides. We have established that **21** – **23** will indeed decarboxylate at higher temperatures and at the same time trifluoromethylate aryl halides. In aryl halide solvent, the ligated copper complexes **21** - **23** outperformed "ligandless" copper iodide. However, in DMA solvent, the ligated copper complexes did not afford any enhancement of yields over the known decarboxylation chemistry of copper salts. With these new complexes and data in hand, we are set to systematically explore the effects of additives and ligand modifications on the facility and scope of decarboxylative trifluoromethylations with the ultimate goal of performing reactions catalytic in copper. These results have been published in *J. Fluorine Chem.*[89]

Scheme 3

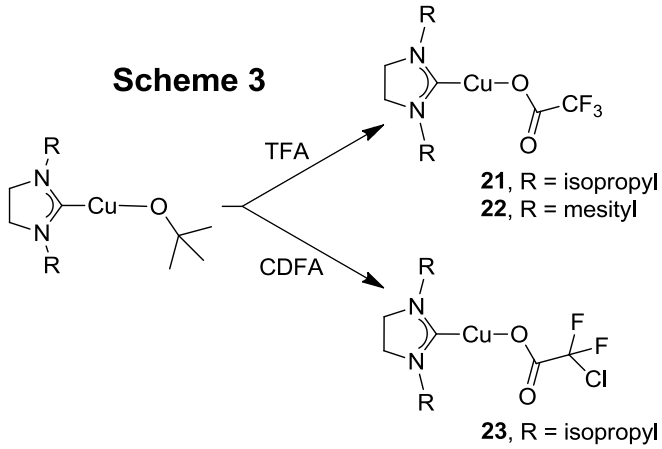

d) Electrocatalytic perfluoroalkylations. In collaboration with Yulia Budnikova from Kazan, Russia, we have developed a new electrocatalytic process that exploits the reactivity of our four-coordinate [(terpyridine)Ni-Br] complex. Scheme 4 highlights the results of these studies. We found that electrogenerated [(terpyridine)Ni-Br] efficiently reduces perfluoroalkyl halides to generate perfluoroalkyl radicals, which then go on to attack olefins. If no other substrate is added, new dimeric products are formed. If hydrogen atom sources are added, we can efficiently generate the monomer. These reactions have the potential of generating a new stereocenter in a perfluoroalkylated product, and future work will focus on developing an asymmetric version of this reaction. These results have recently been published in *Dalton Transactions*.[90]

Scheme 4

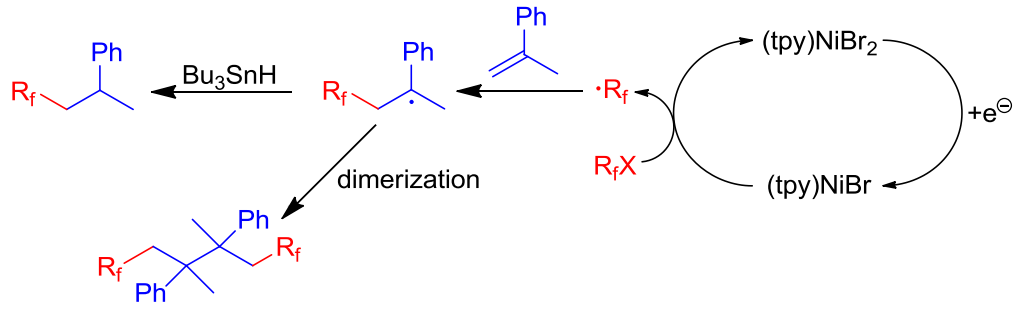

References:

(1) Zhou, J.; Fu, G. C. *J. Amer. Chem. Soc.* **2003**, *125*, 14726.
(2) Anderson, T. J.; Jones, G. D.; Vicic, D. A. *J. Amer. Chem. Soc.* **2004**, *126*, 8100.
(3) Jones, G. D.; Martin, J. L.; McFarland, C.; Allen, O. R.; Hall, R. E.; Haley, A. D.; Brandon, R. J.; Konovalova, T.; Desrochers, P. J.; Pulay, P.; Vicic, D. A. *J. Amer. Chem. Soc.* **2006**, *128*, 13175.
(4) Jones, G. D.; McFarland, C.; Anderson, T. J.; Vicic, D. A. *Chem. Commun.* **2005**, 4211.
(5) Jones, G. D.; Vicic, D. A.; unpublished results.
(6) Gong, H.; Sinisi, R.; Gagne, M. R. *J. Am. Chem. Soc.* **2007**, *129*, 1908.
(7) Gong, H.; Gagne, M. R. *J. Amer. Chem. Soc.* **2008**, *130*, 12177.
(8) Lin, X.; Phillips, D. L. *J. Org. Chem.* **2008**, *73*, 3680.
(9) Phapale, V. B.; Bunuel, E.; Garcia-Iglesias, M.; Cardenas, D. J. *Angew. Chem., Int. Ed.* **2007**, *46*, 8790.
(10) Tyree, W. S.; Vicic, D. A.; Piccoli, P. M. B.; Schultz, A. J. *Inorg. Chem.* **2006**, *45*, 8853.
(11) Vicic, D. A.; Anderson, T. J.; Cowan, J. A.; Schultz, A. J. *J. Amer. Chem. Soc.* **2004**, *126*, 8132.
(12) Bau, R.; Drabnis, M. H. *Inorg. Chim. Acta* **1997**, *259*, 27.
(13) Bau, R.; Teller, R. G.; Kirtley, S. W.; Koetzle, T. F. *Acc. Chem. Res.* **1979**, *12*, 176.
(14) Macchi, P.; Donghi, D.; Sironi, A. *J. Amer. Chem. Soc.* **2005**, *127*, 16494.
(15) Dubinina, G. G.; Furutachi, H.; Vicic, D. A. *J. Amer. Chem. Soc.* **2008**, *130*, 8600.
(16) Wiemers, D. M.; Burton, D. J. *J. Am. Chem. Soc.* **1986**, *108*, 832.
(17) Chang, Y.; Cai, C. *Chin. Chem. Lett.* **2005**, *16*, 1313.
(18) Chang, Y.; Cai, C. *Chem. Lett.* **2005**, *34*, 1440.
(19) Chang, Y.; Cai, C. *Huaxue Shiji* **2005**, *27*, 453.
(20) Chang, Y.; Cai, C. *Journal of Fluorine Chemistry* **2005**, *126*, 937.
(21) Chang, Y.; Cai, C. *Jingxi Huagong* **2005**, *22*, 311.
(22) Chang, Y.; Cai, C. *Tetrahedron Letters* **2005**, *46*, 3161.

(23) Process Research chemists from industry claim in private discussions that Ruppert's reagent is far too expensive to be part of a commercially viable synthetic route.
(24) Drakesmith, F. G. *Topics in Current Chemistry* **1997**, *193*, 197.
(25) Goossen, L. J.; Deng, G.; Levy, L. M. *Science (Washington, DC, United States)* **2006**, *313*, 662.
(26) Cookson, P. G.; Deacon, G. B. *Australian Journal of Chemistry* **1972**, *25*, 2095.
(27) Dankwardt, J. W. *Journal of Organometallic Chemistry* **2005**, *690*, 932.
(28) Gavryushin, A.; Kofink, C.; Manolikakes, G.; Knochel, P. *Tetrahedron* **2006**, *62*, 7521.
(29) Yoshikai, N.; Mashima, H.; Nakamura, E. *J. Amer. Chem. Soc.* **2005**, *127*, 17978.
(30) Hirano, K.; Fujita, K.; Yorimitsu, H.; Oshima, K. *Synlett* **2005**, 1787.
(31) Han, R.; Hillhouse, G. L. *J. Am. Chem. Soc.* **1997**, *119*, 8135.
(32) Lin, B. L.; Clough, C. R.; Hillhouse, G. L. *J. Am. Chem. Soc.* **2002**, *124*, 2890.
(33) Ciszewski, J. T.; Mikhaylov, D. Y.; Holin, K. V.; Kadirov, M. K.; Budnikova, Y. H.; Sinyashin, O.; Vicic, D. A. *Inorg. Chem.* **2011**, *50*, 8630.
(34) Kieltsch, I.; Dubinina, G. G.; Hamacher, C.; Kaiser, A.; Torres-Nieto, J.; Hutchison, J. M.; Klein, A.; Budnikova, Y.; Vicic, D. A. *Organometallics* **2010**, *29*, 1451.
(35) Connelly, N. G.; Geiger, W. E. *Chem. Rev. (Washington, D. C.)* **1996**, *96*, 877.
(36) Carmona, E.; Gonzalez, F.; Poveda, M. L.; Atwood, J. L.; Rogers, R. D. *J. Chem. Soc., Dalton Trans.* **1981**, 769.
(37) Jacob, K.; Thiele, K. H.; Geyer, C.; Welde, G. *Z. Anorg. Allg. Chem.* **1980**, *462*, 177.
(38) Kohara, J.; Yamamoto, T.; Yamamoto, A. *Journal of Organometallic Chemistry* **1980**, *192*, 265.
(39) Koo, K.; Hillhouse, G. L. *Organometallics* **1995**, *14*, 4421.
(40) Saito, T.; Uchida, Y.; Misono, A.; Yamamoto, A.; Morifuji, K.; Ikeda, S. *J. Amer. Chem. Soc.* **1966**, *88*, 5198.
(41) Takahashi, S.; Suzuki, Y.; Sonogashira, K.; Hagihara, N. *Journal of the Chemical Society, Chemical Communications* **1976**, 839.
(42) Tsou, T. T.; Kochi, J. K. *J. Am. Chem. Soc.* **1978**, *100*, 1634.
(43) Yamamoto, T.; Abla, M. *J. Organomet. Chem.* **1997**, *535*, 209.
(44) Yamamoto, T.; Nakamura, Y.; Yamamoto, A. *Bull. Chem. Soc. Jpn.* **1976**, *49*, 191.
(45) Yamamoto, T.; Yamamoto, A.; Ikeda, S. *J. Amer. Chem. Soc.* **1971**, *93*, 3350.
(46) Klein, A.; Kaiser, A.; Sarkar, B.; Wanner, M.; Fiedler, J. *Eur. J. Inorg. Chem.* **2007**, 965.
(47) Dinjus, E.; Walther, D.; Kirmse, R.; Stach, J. *J. Organomet. Chem.* **1980**, *198*, 215.
(48) Kirmse, R.; Stach, J.; Dinjus, E.; Walther, D. *Z. Chem.* **1980**, *20*, 213.
(49) Walther, D.; Dinjus, E.; Ihn, W.; Schade, W. *Z. Anorg. Allg. Chem.* **1979**, *454*, 11.
(50) Chaudhury, N.; Kekre, M. G.; Puddephatt, R. J. *J. Organometal. Chem.* **1974**, *73*, C17.
(51) Davis, J. L.; Arndtsen, B. A. *Organometallics* **2011**, *30*, 1896.
(52) Han, R.; Hillhouse, G. L. *J. Am. Chem. Soc.* **1998**, *120*, 7657.
(53) Keim, W.; Berger, M.; Eisenbeis, A.; Kadelka, J.; Schlupp, J. *J. Mol. Catal.* **1981**, *13*, 95.

(54) Lin, B. L.; Clough, C. R.; Hillhouse, G. L. *J. Am. Chem. Soc.* **2002**, *124*, 2890.
(55) Matsunaga, P. T.; Hess, C. R.; Hillhouse, G. L. *J. Am. Chem. Soc.* **1994**, *116*, 3665.
(56) Matsunaga, P. T.; Mavropoulos, J. C.; Hillhouse, G. L. *Polyhedron* **1995**, *14*, 175.
(57) Yamamoto, A.; Morifuji, K.; Ikeda, S.; Saito, T.; Uchida, Y.; Misono, A. *J. Am. Chem. Soc.* **1965**, *87*, 4652.
(58) Yamamoto, T. *J. Chem. Soc., Chem. Commun.* **1978**, 1003.
(59) Yamamoto, T.; Kohara, T.; Osakada, K.; Yamamoto, A. *Bull. Chem. Soc. Jpn.* **1983**, *56*, 2147.
(60) Yamamoto, T.; Kohara, T.; Yamamoto, A. *Chem. Lett.* **1976**, 1217.
(61) Yamamoto, T.; Kohara, T.; Yamamoto, A. *Bull. Chem. Soc. Jpn.* **1981**, *54*, 2161.
(62) Yamamoto, T.; Kohara, T.; Yamamoto, A. *Bull. Chem. Soc. Jpn.* **1981**, *54*, 1720.
(63) Yamamoto, T.; Yamamoto, A. *Chem. Lett.* **1978**, 615.
(64) Bialek, M.; Cramail, H.; Deffieux, A.; Guillaume, S. M. *Eur. Polym. J.* **2005**, *41*, 2678.
(65) Kaul, E.; Senkovskyy, V.; Tkachov, R.; Bocharova, V.; Komber, H.; Stamm, M.; Kiriy, A. *Macromolecules (Washington, DC, U. S.)* **2010**, *43*, 77.
(66) Kiriy, A.; Senkovskyy, V. *Polym. Prepr. (Am. Chem. Soc., Div. Polym. Chem.)* **2010**, *51*, 233.
(67) Senkovskyy, V.; Beryozkina, T.; Bocharova, V.; Tkachov, R.; Komber, H.; Lederer, A.; Stamm, M.; Severin, N.; Rabe, J. P.; Kiriy, A. *Macromol. Symp.* **2010**, *291-292*, 17.
(68) Senkovskyy, V.; Beryozkina, T.; Komber, H.; Lederer, A.; Stamm, M.; Kiriy, A. *Polym. Prepr. (Am. Chem. Soc., Div. Polym. Chem.)* **2008**, *49*, 630.
(69) Senkovskyy, V.; Kaul, E.; Tkachov, R.; Komber, H.; Stamm, M.; Kiriy, A. *Polym. Prepr. (Am. Chem. Soc., Div. Polym. Chem.)* **2010**, *51*, 367.
(70) Senkovskyy, V.; Tkachov, R.; Beryozkina, T.; Komber, H.; Oertel, U.; Horecha, M.; Bocharova, V.; Stamm, M.; Gevorgyan, S. A.; Krebs, F. C.; Kiriy, A. *J. Am. Chem. Soc.* **2009**, *131*, 16445.
(71) Tkachov, R.; Senkovskyy, V.; Horecha, M.; Oertel, U.; Stamm, M.; Kiriy, A. *Chem. Commun.* **2010**, *46*, 1425.
(72) Tkachov, R.; Senkovskyy, V.; Komber, H.; Sommer, J.-U.; Kiriy, A. *J. Am. Chem. Soc.* **2010**, *132*, 7803.
(73) Tkachov, R.; Senkovskyy, V.; Oertel, U.; Synytska, A.; Horecha, M.; Kiriy, A. *Macromol. Rapid Commun.* **2010**, *31*, 2146.
(74) Yamamoto, T.; Konagaya, S.; Yamamoto, A. *J. Polym. Sci., Polym. Lett. Ed.* **1977**, *15*, 729.
(75) Yamamoto, T.; Konagaya, S.; Yamamoto, A. *J. Polym. Sci., Polym. Lett. Ed.* **1978**, *16*, 7.
(76) Durandetti, M.; Perichon, J. *Synthesis* **2004**, 3079.
(77) Budnikova, Y. G.; Kargin, Y. M.; Sinyashin, O. G. *Mendeleev Communications* **1999**, 193.
(78) Budnikova, Y. H.; Perichon, J.; Yakhvarov, D. G.; Kargin, Y. M.; Sinyashin, O. G. *J. Organomet. Chem.* **2001**, *630*, 185.
(79) de, F. K. W. R.; Navarro, M.; Leonel, E.; Durandetti, M.; Nedelec, J.-Y. *J. Org. Chem.* **2002**, *67*, 1838.
(80) Gosmini, C.; Nedelec, J. Y.; Perichon, J. *Tetrahedron Lett.* **1999**, *41*, 201.

(81) Cundy, C. S.; Green, M.; Stone, F. G. A. *Journal of the Chemical Society [Section] A: Inorganic, Physical, Theoretical* **1970**, 1647.

(82) Gasafi-Martin, W.; Oberendfellner, G.; von, W. K. *Canadian Journal of Chemistry* **1996**, *74*, 1922.

(83) Hoberg, H.; Guhl, D. *J. Organomet. Chem.* **1989**, *378*, 279.

(84) Klein, A.; Feth, M. P.; Bertagnolli, H.; Zalis, S. *Eur. J. Inorg. Chem.* **2004**, 2784.

(85) Tucci, G. C.; Holm, R. H. *J. Amer. Chem. Soc.* **1995**, *117*, 6489.

(86) Yang, D. S.; Bancroft, G. M.; Dignard-Bailey, L.; Puddephatt, R. J.; Tse, J. S. *Inorg. Chem.* **1990**, *29*, 2487.

(87) Teverovskiy, G.; Surry, D. S.; Buchwald, S. L. *Angew. Chem., Int. Ed.* **2011**, *50*, 7312.

(88) Zhang, C.-P.; Vicic, D. A. *J. Am. Chem. Soc.*, Ahead of Print.

(89) McReynolds, K. A.; Lewis, R. S.; Ackerman, L. K. G.; Dubinina, G. G.; Brennessel, W. W.; Vicic, D. A. *J. Fluorine Chem.* **2010**, *131*, 1108.

(90) Mikhaylov, D.; Gryaznova, T.; Dudkina, Y.; Khrizanphorov, M.; Latypov, S.; Kataeva, O.; Vicic, D. A.; Sinyashin, O. G.; Budnikova, Y. *Dalton Transactions* **2012**, *41*, 165.